



**HAL**  
open science

## Flickering of a diffusion flame: An innovative way of stabilization by a mechanical actuator

Ahmad Sayed-Kassem, Pascale Gillon, Mahmoud Idir, Virginie Gilard

### ► To cite this version:

Ahmad Sayed-Kassem, Pascale Gillon, Mahmoud Idir, Virginie Gilard. Flickering of a diffusion flame: An innovative way of stabilization by a mechanical actuator. *International Communications in Heat and Mass Transfer*, 2022, 139, pp.106475. 10.1016/j.icheatmasstransfer.2022.106475 . hal-03880220

**HAL Id: hal-03880220**

**<https://cnrs.hal.science/hal-03880220v1>**

Submitted on 5 Jul 2024

**HAL** is a multi-disciplinary open access archive for the deposit and dissemination of scientific research documents, whether they are published or not. The documents may come from teaching and research institutions in France or abroad, or from public or private research centers.

L'archive ouverte pluridisciplinaire **HAL**, est destinée au dépôt et à la diffusion de documents scientifiques de niveau recherche, publiés ou non, émanant des établissements d'enseignement et de recherche français ou étrangers, des laboratoires publics ou privés.

# Flickering of a diffusion flame: an innovative way of stabilization by a mechanical actuator

*Ahmad Sayed-Kassem<sup>a,b\*</sup>, Pascale Gillon<sup>c</sup>, Mahmoud Idir<sup>a</sup>, Virginie Gilard<sup>a,b</sup>*

- a. CNRS-INSIS, ICARE Laboratory, 1C Avenue de la Recherche Scientifique, 45071 Orléans, Cedex2, France
- b. Université d'Orléans, IUT, 45067 Orléans, France
- c. CNRS and Université de Nantes, GEPEA Laboratory, 37 Boulevard de l'Université, 44600 Saint-Nazaire, France

\* **Ahmad Sayed-Kassem:** [ahmad.sayed-kassem@outlook.com](mailto:ahmad.sayed-kassem@outlook.com)

## Highlights

- Flickering instability of diffusion flame has been studied by flame imaging and temporal recording of transmitted signal.
- Three different regimes of instability are identified depending on fuel flowrate.
- A flickering frequency of 11 Hz is measured for ethylene diffusion flame with a “pinch-off” velocity of 1450 mm/s.
- The controllability of flickering by a mechanical stabilizer is proved for methane and ethylene diffusion flames.

## Abstract

Flickering is an oscillating instability of a diffusion flame. An experimental study has been performed on two different diffusion flame of methane and ethylene to elucidate flickering instability and controlling it by the mean of a mechanical stabilizer. Flame imaging and temporal evolution of transmitted signal methods have been employed to monitor the flame behavior and measure flickering frequency. Three different regimes of stability are identified: stable, transient, and full unstable. The measured flickering frequency of ethylene flame is 11 Hz and it is demonstrated to be independent of fuel jet velocity. The calculated vortex mean velocity is 500 mm/s and 800 mm/s without and with “pinch-off” formation respectively and the “pinch-off” velocity is around 1450 mm/s. Moreover, the ability of a mechanical actuator to stabilize the flame has been demonstrated for methane and ethylene. The experiment reveals the existence of a limit of stabilizing height at each flowrate. However, positioning stabilizer below the burner shows a limited effect. Numerical simulation shows a smoother effect of stabilizer on air streamlines around the flame limiting the action of vortex on the flame. These results prove that flickering instability could be suppressed by only controlling the air surrounded the flame.

**Keywords:** Diffusion flame, flickering, mechanical stabilizer, methane, ethylene

## 1. Introduction

A jet flame generates a strong temperature gradient between combustion gas and ambient air ( $\Delta T \sim 1800$  K). This strong variation creates a density gradient and a shear layer near the flame front and generates the “Kelvin-Helmholtz” instability, called “Flickering”. Thus, flickering is a buoyant type instability. This instability could be strong enough to cut the flame and form a second flame pocket called “pinch-off”.

Flickering has been widely studied by researchers in the combustion community and the impact of different factors on flickering instability has been demonstrated. First, a co-flow acts on flickering characteristics as reported in [1–6]. Recently, Piemsinlapakunchon and Paul [7] performed a numerical study to elucidate the effect of gas composition (syngas) and air co-flow on flame flickering. They observed an enhancement in flame behavior with higher co-flow rate until the suppression of the instability. The authors also revealed the impact of gas composition on flame stability: H<sub>2</sub> and CH<sub>4</sub> promote flame fluctuation rather than CO and CO<sub>2</sub>. The same result on co-flow impact was experimentally validated by Raju et al. [8]. They studied LPG flame behavior at different co-flow rate using photomultiplier tube time signal recording and image processing techniques. Additionally, other flow conditions could affect flame stability as indicated in [9–17]. Chi et al. [18,19] studied the interaction of three flickered flame with different arrangement. Different dynamical modes have been distinguished, and the main conclusion is such interaction could suppress instability (flickering death mode) or promote it (rotation mode, in-phase mode). In the same way, Hao et al. [20] studied the interaction of two candle flames. Here, several synchronization states have been elucidated with different modes (in-phase, anti-phase and incoherent). An example on how an instability could be triggered is the acoustic perturbation [21–24]. Ahn et al. [25] used acoustic excitation to analyze pinch-off flame structure and NO<sub>x</sub> emissions in H<sub>2</sub>/CH<sub>4</sub> premixed flame. The results show an increase in pollutant formation (NO<sub>x</sub> and CO) with excitation frequencies below 60 Hz. Other publications [21,24,26–28] demonstrate the promoting effect of instability on soot production (~4x). This effect could be boosted by pinch-off formation (~7x). Therefore, stabilizing a flame has a positive impact in terms of pollutant emissions (lowering soot formation and NO<sub>x</sub> and CO emissions) and combustion efficiency (a stable combustion is more efficient).

Different studies have been carried out in order to control flickering and extend stability domain of the flame. Flickering instability is dampened in the presence of a higher oxygen content, as reported in [29–33]. The effect of an external magnetic field was studied by 50 Gillon et al. [34]. The authors observed a stability enhancement of a methane lifted flame submitted to a magnetic field. This behavior was explained by the interference of magnetic convection with the air in the vicinity of the flame. Gillon et al. [35] explained the impact of a DC vertical electric field on ethylene diffusion flame stability by an ionic wind, which 55 opposes the vortex and enhances flame behavior. The author also reported a reduction of mean soot volume fraction at the flame axis. In the same way, Xiong et al. [36] investigated the effect of a DC electric field on M-shape premixed Bunsen flame. They concluded that a DC electric field could stabilize a flickered flame, and the important parameter is the direction of electric body force.

60 Unlike the last presented studies, in this work, we propose to elucidate the effect of a passive actuator on the stability of a flickered flame. A passive actuator could act on the flame without interfering to any external action (this external action could be for example electric field, magnetic field, acoustic wave, etc.). Such actuator is operationally free and relatively simple. Here, the action of a mechanical actuator on an unstable flame is investigated. Two 65 different fuels have been used: methane and ethylene to validate the mechanical stabilizer impact. Flame imaging and time recorded transmitted signal have been employed in order to monitor flame behavior and measure flickering frequency. Different conditions have been tested to elucidate the impact of a mechanical stabilizer and its ability to control flame stability.

## 70 2. Experiment

### 2.1. Experimental conditions

Two different burners were used in this study. The first one is the methane burner, made from a stainless-steel tube with an internal diameter of 10 mm. The second one is the ethylene burner. It is formed from two concentric stainless parts: a 0.1 mm thickened tube with an  
75 internal diameter of 9.8 mm and an external tube of 30 mm of diameter. The fuel is injected in the central tube and since the objective of this study is to study the flame stability without any other effect, no co-flow was set in the outer tube.

Methane and ethylene were injected with different flow rates. Methane flowrates swept in this study are between 1.36 cm<sup>3</sup>/s and 14.6 cm<sup>3</sup>/s, corresponding to a Reynold's number  
80 between 10.6 and 112.7. The injection conditions for methane are presented in Table 1.

**Table 1.** Methane injection conditions

<b>Flowrate</b> (cm <sup>3</sup> /s)	1.36	1.81	2.47	3.57	4.02	5.12	6.23	10.2	14.6
<b>Injection velocity</b> (cm/s)	1.7	2.3	3	4.5	5	6.5	8	13	19
<b>Reynolds' number</b>	10	13.6	17.8	26.7	29.7	38.6	47.5	77.1	112.7

For the ethylene, flowrate was varied from 2.18 cm<sup>3</sup>/s to 5.97 cm<sup>3</sup>/s, corresponding to a Reynold's number between 355 and 968 as presented in the Table 2. For simplicity, each flowrate is indexed by Qi (Q<sub>1</sub> is for the lowest flowrate).

85 **Table 2.** Ethylene injection conditions





<b>Flowrate</b>	$Q_1$	$Q_2$	$Q_3$	$Q_4$	$Q_5$	$Q_6$	$Q_7$
<b>Value</b> (cm <sup>3</sup> /sec)	2.18	2.66	3.1	3.45	3.82	4.98	5.97
<b>Injection velocity</b> (cm/sec)	2.9	3.53	4.12	4.58	5	6.6	7.92
<b>Reynolds' number</b>	355	432	504	560	611	807	968

## 2.2. Mechanical stabilizers

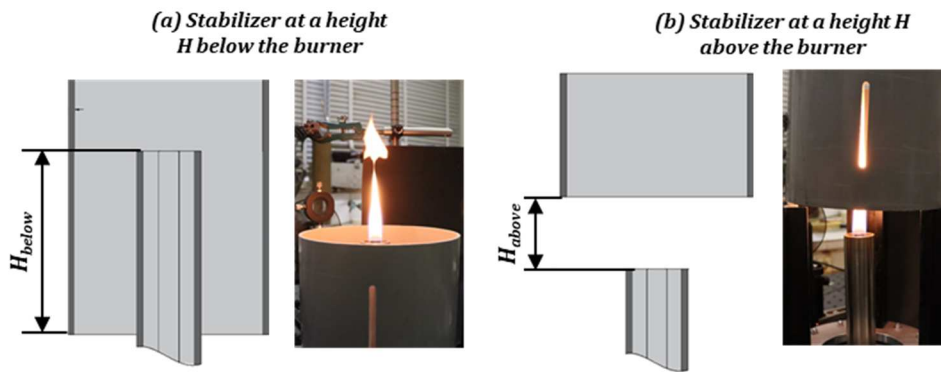
A mechanical stabilizer consists of a cylindrical tube with defined length and diameter. mounted at a fixed position from the burner exit. Different stabilizers were employed in this study. The Table 3 shows the geometric characteristics of employed stabilizers with the corresponding images.

**Table 3.** Geometric characteristics of stabilizers and corresponding images

<b>Stabilizer</b>	1	1*	2	3	4
<b>Length</b> (mm)	120	220	130	214	300
<b>Diameter</b> (mm)	94	94	155	205	44

Different positions could be selected for the stabilizer below the burner (Figure 1.(a)) or above (Figure 1.(b)). Here, the burner tip is taken as reference (height = 0 mm).



95

Figure 1. Stabilizer positions as respect to the burner: (a) at a height  $H$  below the burner. (b) at a height  $H$  above the burner

### 2.3. Flame temporal evolution

The temporal evolution of the flame was monitored by the mean of a camera with a 25 Hz of  
 100 a frame rate. Videos were recorded at different states of the flame in order to be processed by  
 the mean of Matlab video processing functions. The flame length corresponds to the  
 luminous one. calculating by considering the distance between fuel exit and flame tip with a  
 minimal pixel intensity of 30.

Flickering frequency was determined by measuring the temporal evolution of the transmitted  
 105 signal. For this purpose, a He-Ne laser was used with a photodiode connected to an  
 acquisition card, as presented by the Figure 2. All signals were measured at a fixed height  
 above the burner (30 mm) with an acquisition frequency of 40 kHz and an acquisition time of  
 25 s. Then, a Fast Fourier Transform was applied in order to calculate the characteristic  
 frequency of the instability.



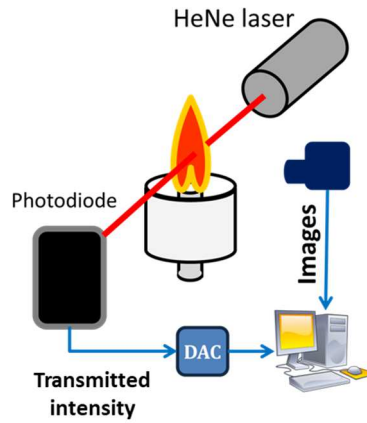


**Figure 2.** Flame monitoring techniques set-up

### 3. Results

#### 3.1. Methane diffusion flame

##### 3.1.1. Stability regimes

115 Figure 3 shows the instantaneous evolution of flame length at different flowrate. Three different behaviors could be identified from the Figure 3:

- The flame is stable, and the length remains constant during the time for methane flowrates of 1.36 and 1.81 cm<sup>3</sup>/s.
  - The flame exhibits two phases at 2.47 cm<sup>3</sup>/s: an unstable phase when the flame length oscillates during the time (phases between 0 s and 40 s and between 80 s and 130 s). And a stable regime when the flame length remains almost unchangeable (phase between 40 s and 80 s).
  - The flame is always unstable, and the flame length oscillates for higher methane flowrates.
- 120

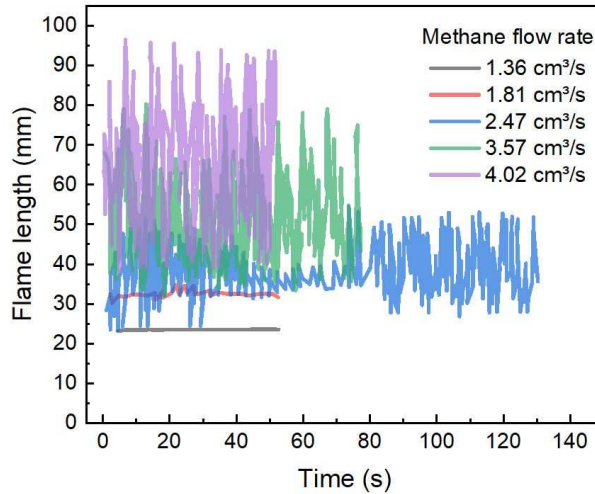


**Figure 3.** Methane flame length evolution as function of time at different flowrates

3.1.2. Mechanical stabilization

Figure 4 displays the flame length evolution with the root mean square (RMS) as function of methane flow rate without or with the mechanical stabilizer 1 mounted at two different positions (46 and 56 mm above the burner). The flame images correspond to a methane flowrate at 5.1 cm<sup>3</sup>/s with two positions of stabilizer 1.

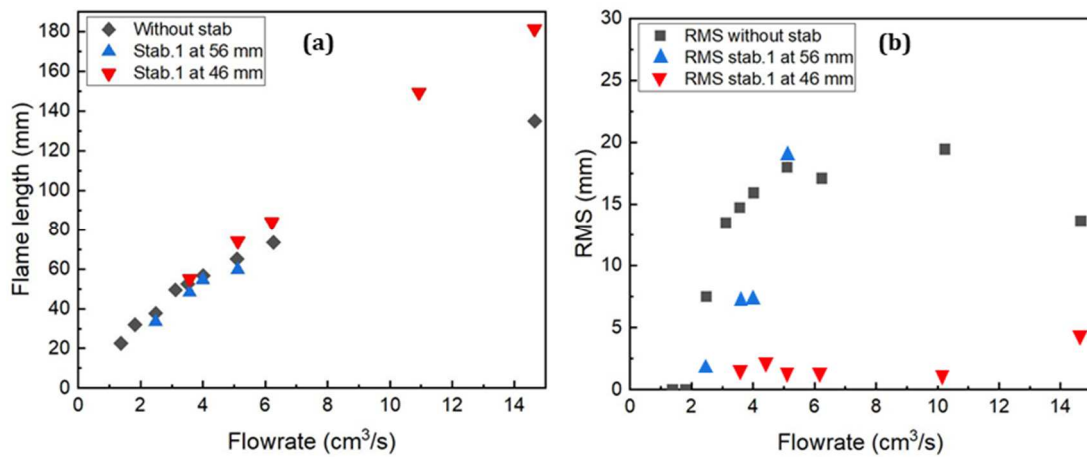


**Figure 4.** (a) Mean flame length evolution and (b) RMS as function of methane flowrate at different conditions

As could be remarked in the plot, the RMS of flame length is diminished under the effect of stabilizer 1 placed at 56 mm of height until 5.1 cm<sup>3</sup>/s of methane flowrate where the

instability reappears. Whereas, with a position of 46 mm, the instability is almost suppressed even with higher flowrates. These results validate the stabilizing effect of a mechanical actuator and highlight the position effect.

140 In order to elucidate the effect of a stabilizer and its position on the flame behavior, a series of experiment was performed at different flowrates using the stabilizer 1 and 1\*. The results are presented in the Figure 5(a-b) as a form of a stability diagram.

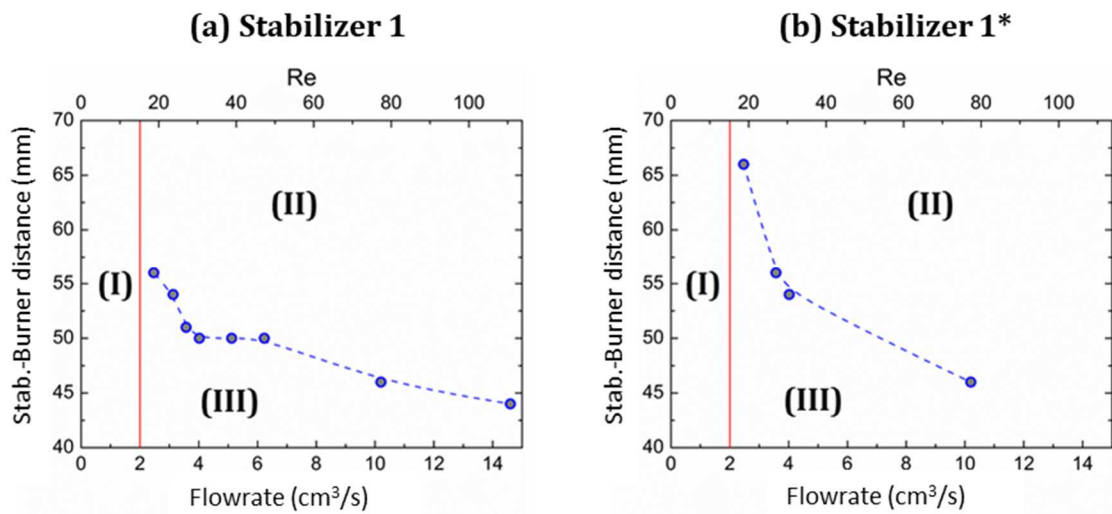


**Figure 5.** Stability diagrams of stabilizers 1 and 1\*. Zone (I) is the stable zone, zone (II)

145 corresponds to the unstable one and zone (III) refers to the extended stability zone

Three different zones could be distinguished in the stability diagram:

- Zone (I): corresponds to the stable zone. Under this limit (2 cm<sup>3</sup>/s in this case), the flame is always stable.
- Zone (II): corresponds to the unstable zone. The flame is always unstable even with 150 employing a mechanical stabilizer.
- Zone (III): corresponds to the extended stability zone. The flame is stabilized by the virtue of a mechanical stabilizer.

The two plots of the Figure 5 point out the effect of stabilizer length: A longer stabilizer is more efficient specifically for medium flowrates (just above stability limit): at 2.1 cm<sup>3</sup>/s. the stabilization position of stabilizer 1 is about 55 mm. lower than that of stabilizer 1\* (about 65 mm).

### **3.2. Ethylene diffusion flame**

#### *3.2.1. Stability regimes*

Figure 6 represents the luminous flame length evolution as function of ethylene flow rate at different states. Three states are presented in this figure: the first state refers to the stable flame marked by a filled dot (flames (a). (d) and (g); the flame (g) was stabilized by the mean of a mechanical stabilizer with an orifice (stabilizer 2)). The second state corresponds to the minimal flame length and is presented by the upward-pointing triangle (flames (b) and (e)). And the third state designates the highest flame length and is presented by the downward-pointing triangle (flames (c) and (f)). The images (a-g) correspond to the different point in the plot.

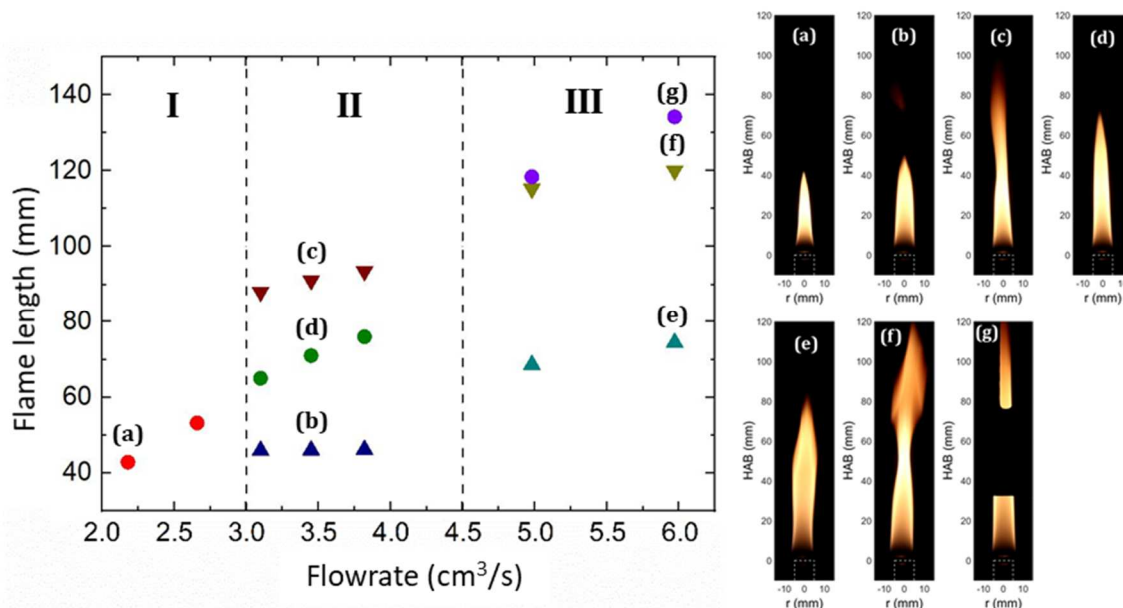


**Figure 6.** Flame length evolution as function of flowrate. The filled dots correspond to stable flames (a, d, and g), the upward-pointing triangles refer to minimal length flames (b and e) and the downward-pointing triangles present the flames with highest length (c and f). The region I, II and III refer respectively to stable, transient, and unstable regimes.

170

From the Figure 6, three different regimes could be distinguished, similarly to methane diffusion flame:

- The regime (I) is the stable one: the flame maintains its shape and no temporal variation is observed (flame (a)).
- The regime (II) corresponds to the transient regime: the flame state varies between stable (flame (d)) and unstable (flames (b) and (c)).
- The regime (III) represents the fully unstable regime: the flame is always unstable for higher values of ethylene flow rate (flames (e) and (f)).

175

### 180 3.2.2. Flickering frequency

Figure 7 (a) and (c) represent the temporal evolution of transmitted intensity for the transient and fully unstable regimes, respectively. As presented above, the transmitted signal shows

two zones corresponding to the stable and the unstable times (Figure 7 (a)). Whereas, this signal is always unstable for higher flowrates, highlighting the persistence of the instability.

185 Figure 7 (b) and (d) depict the FFT of transmitted signals at different flow rates. A frequency of 11 Hz was detected for all cases independently from fuel flowrate. This result is consistent with the literature: the flickering instability has been shown to be independent from the fuel flow rate and it varies from 10 to 20 Hz, depending on the injector diameter ( $f \propto (g/d)^{0.5}$  where  $f$  is the flickering frequency,  $g$  is the gravitational acceleration and  $d$  is the injection diameter) [28,29]. Moreover, ethylene diffusion flame instability follows St-Fr correlation expressed by Sato et al. [37] as  $St = 0.35Fr^{-0.5}$  where St and Fr correspond respectively to Strouhal and Froude numbers.

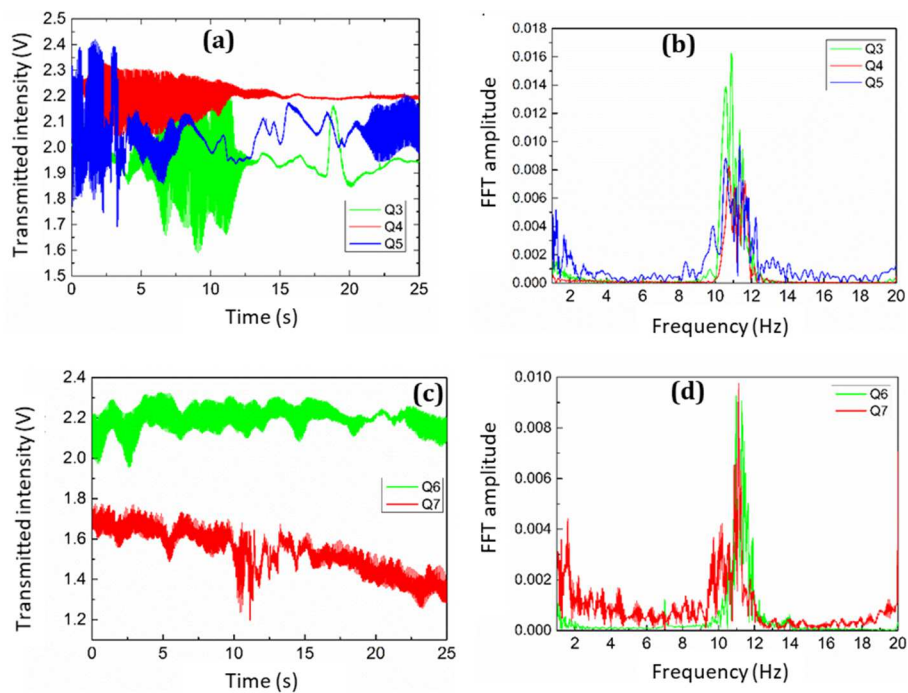


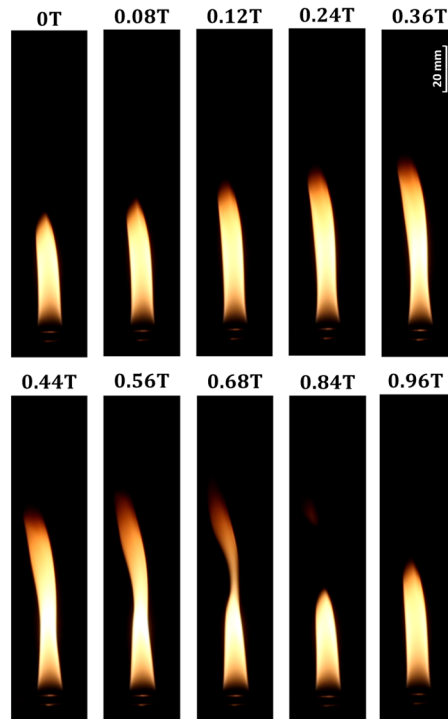
**Figure 7.** Transmitted signal evolution and FFT at different ethylene flowrate. (a) and (b)

195 refer to the transient regime and (c) and (d) to the fully unstable regime

The images of Figure 8 display the temporal evolution of the flame during an instability phase of the transient regime (3.45 cm<sup>3</sup>/s of ethylene flowrate). T corresponds to the

instability period determined by FFT (91 ms). From these images, different remarks could be noted:

- 200
- The instability is not strong enough to cut the flow and form the pinch-off. Only temporal variation of the flame length is detected.
  - A temporal dissymmetry of the flame length variation is observed: the time separated the highest flame to the shorter one does not match to a half period ( $0.84T - 0.56T = 0.28T$ ). The same observation was noted by Kashiff et al. [38].
- 205
- Since the vortex starts near the burner exit (when the flame has its minimal length) and continue to act on the flame until cutting it during the period  $T$ , the mean axial velocity of the vortex could be estimated by 506 mm/s ( $\approx f \times L_{\min}$ ). Here,  $L_{\min}$  corresponds to the minimal length measured during a period of instability. In this case, it corresponds to the length detected at  $0.84T$ .



210

**Figure 8.** Flame temporal evolution at  $3.45 \text{ cm}^3/\text{s}$  of ethylene flowrate during a period of instability  $T$  ( $T = 1/f$ ).

Figure 9 represents the images of fully instable flame with an ethylene flowrate of  $5.97 \text{ cm}^3/\text{s}$ .

The red point in the images between  $0.44T$  and  $0.96T$  marks the position of the deflection point induced by the vortex. At this point, flame diameter is minimal due to the vortex action.

215

Different remarks could be noticed:

- Images between  $0T$  and  $0.21T$  show pinch-off formation.
- The temporal deviation, observed in the transient regime, could also be noted here: a delay of  $0.28T$  separates the highest flame from the shortest one.
- The mean axial velocity of the vortex could be estimated by  $814 \text{ mm/s}$  ( $\approx f \times L_{min}$ ).  $L_{min}$  corresponds to the flame length at  $0.08T$ .

220



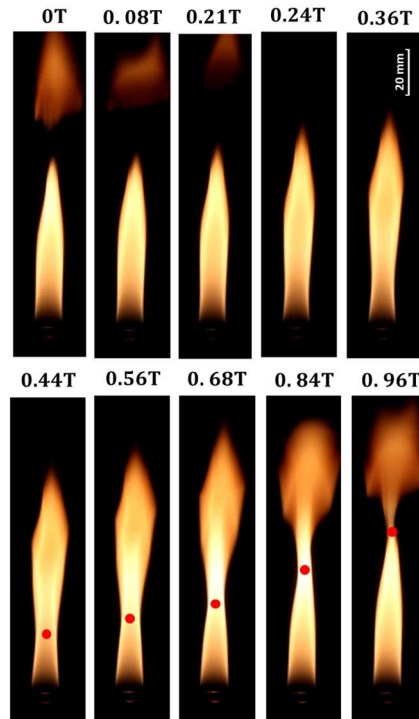


**Figure 9.** Flame temporal evolution at 5.97 cm<sup>3</sup>/s of ethylene flowrate during a period of instability  $T$  ( $T = 1/f$ ). The red dots in the images between 0.44T and 0.96T correspond to the deflection point and indicate vortex position

225

The instantaneous axial velocity of the vortex could be calculated by monitoring the axial position of the deflection point at different moments. These velocities are presented by the Figure 10. The instantaneous velocities were calculated as the ratio of the variation of the deflection point axial position to the temporal variation ( $\approx \Delta h/\Delta t$ .  $h$  is the deflection point axial position and  $t$  is the time).

230

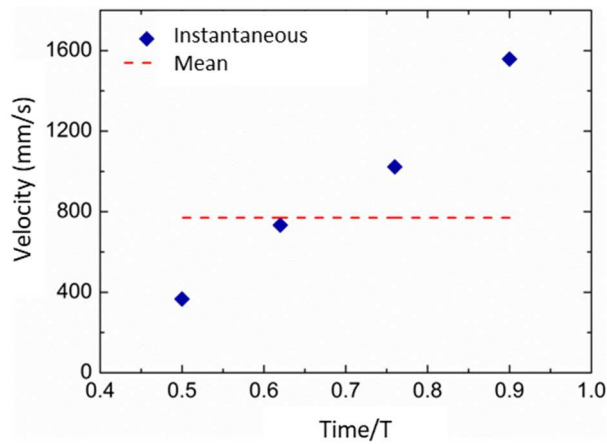


**Figure 10.** Vortex speed evolution at 5.97 cm<sup>3</sup>/s of ethylene flowrate

The red dot line of the Figure 10 represents the mean axial velocity calculated using the instantaneous measurements. This velocity (770 mm/s) is nearly close to the calculated  
 235 velocity using the minimal length (814 mm/s).

The vortex axial velocity becomes more and more important throughout the flame due to the buoyancy effect. This velocity reaches a sufficient value (1450 mm/s) to cut the flame and form the pinch-off. The Contrarily, in the case of transient regime (Q<sub>3</sub>, Q<sub>4</sub> and Q<sub>5</sub>), the flame is too short to accelerate enough the vortex and enter the “pinch-off” regime (mean axial  
 240 velocity~500 mm/s vs~800 mm/s in the case of Q<sub>6</sub> and Q<sub>7</sub>).

The accelerated motion of the vortex could explain the temporal deviation observed in the transient and the unstable regimes. Indeed, the change from a short to a long flame is favored by the heat release, which becomes more and more important as the flame rises and the vortex accelerates under the effect of gravity.

### 245 3.2.3. Mechanical stabilization

In this part, two positions of stabilizer were defined: position 1, where the stabilizer is mounted 85 mm below the burner tip (H= 85 mm in the Figure 1 (a)), and the position 2, where the stabilizer is 35 mm above the burner (H= 35 mm in the Figure 1 (b)).

The Fast Fourier Transform (FFT) of transmitted signal under different conditions and fixed ethylene flowrate ( $Q_4$ , transient regime) is presented by the plots of Figure 11 (a-b). A stabilizer installed at the position 1 appears inefficient to suppress the instability. Whereas, at the position 2, the FFT signal is stable, indicating that the flame is stabilized.

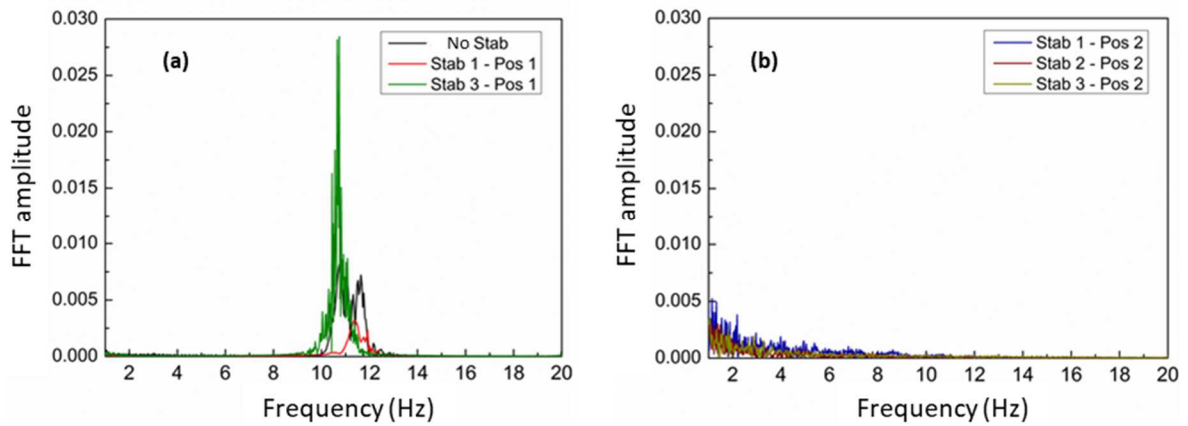


**Figure 11.** FFT of transmitted signal at 3.45 cm<sup>3</sup>/s of ethylene flowrate under different conditions: (a) unstable flame and (b) stabilized flame

The same tendency could be observed with higher flow rate ( $Q_7$ , fully unstable regime) as revealed in the Figure 12 (a-b), except in the case of stabilizer 4 mounted at the position 1. This result could be explained by the higher length of the stabilizer 4, as noted in the section 1. It should be noted that not all stabilizers are presented in the two Figures 11 and 12 due to a problem in positioning or the very narrow diameter (stabilizer 4 at higher flow rate).

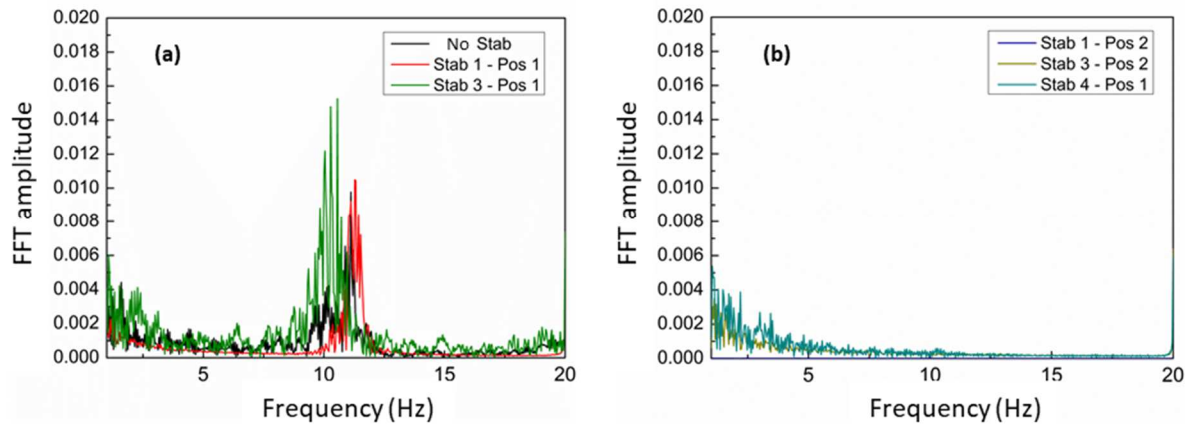


**Figure 12.** FFT of transmitted signal at 5.97 cm<sup>3</sup>/s of ethylene flowrate under different conditions: (a) unstable flame and (b) stabilized flame

### 3.3. Discussion

265 To better understand the stabilizer effect on the external air flow around the flame, numerical calculations were performed simulating three different cases: without a stabilizer and with a stabilizer mounted at two different positions (positions 1 and 2 in the case of ethylene diffusion flame).

Here, the same mathematical model developed in a previous study [39] was employed. The 270 steady-state Navier-Stokes equations of continuity, momentum, energy and species of the 2D axisymmetric configuration were resolved. A laminar flow was assumed with a one-step reaction to calculate the net rate of consumption/ production and ethylene combustion heat release. This model was validated by comparing temperature and velocity profiles to experimental measurements. Since the objective of the calculation is to focus only on the 275 external air flow, the assumption of a steady-state regime was selected. The ethylene flow rate was fixed at 3.45 cm<sup>3</sup>/s without an air co-flow.

All geometric characteristics of the experiment were reproduced by the model, and the boundary conditions were adapted to simulate the real case. The mechanical stabilizer was modeled by an adiabatic wall. The calculation domain for each case with the boundary

280 conditions are presented by the Figure 13. The boundaries 3 and 4 were set to the atmospheric conditions (atmospheric pressure and ambient temperature).

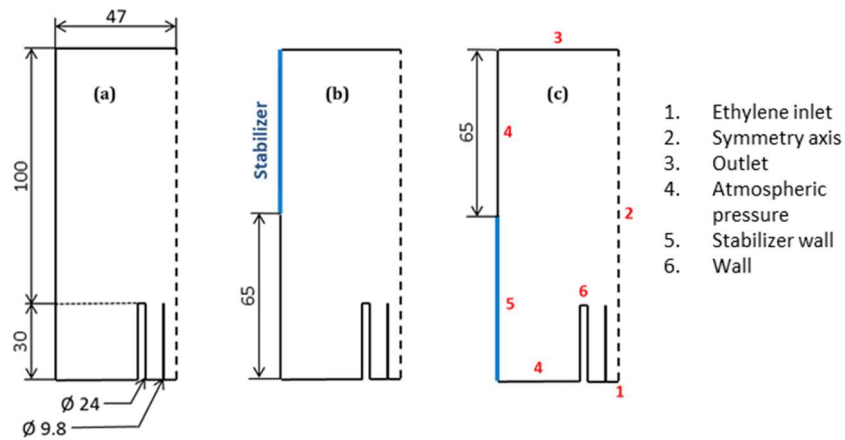
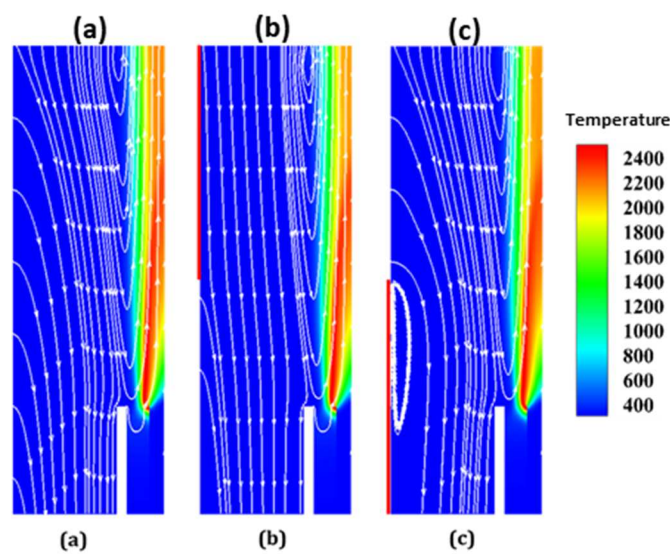


**Figure 13.** Simulated cases with boundary conditions

285 Figure 14 (a-c) represent the air streamlines with the temperature distribution for the three tested cases respectively. When a stabilizer is mounted at Position 2, the interference of the air coming from the atmosphere with the flame is limited comparing to the other two cases. The air streamlines appear smoother and unidirectional. This fact could mitigate the vortex action on the flame and disable the flickering regime.



290 **Figure 14.** Air streamlines with the temperature distribution for the three tested cases

In the case of a stabilizer positioned below the burner exit, the air streamlines continue to interfere with the flame as the reference case. This fact could explain the persistence of instability as revealed in the last section even though the presence of the stabilizer. Nevertheless, the presence of a stabilizer influences the air streamlines that could be longer  
295 and then the instability can be less violent. This effect may explain the decreasing in FFT amplitude observed in the Figure 14 (c).

## Conclusion

In this study, flickering instability of diffusion flame of two different fuel (methane and ethylene) has been studied. A new way of controlling this instability has been proposed by  
300 the mean of a mechanical actuator. Flame imaging and time recording of transmitted signal methods have been employed to monitor the flame instability and measure flickering frequency.

Several observations could be noted from this study and listed as follows:

- Three different regimes of stability are distinguished in methane and ethylene diffusion  
305 flames: a stable regime for lower flow rate, a transition regime for intermediate flow rate and a fully unstable regime for higher flow rate.
- For an unstable ethylene diffusion flame without a pinch-off formation, the mean vortex velocity was measured by 500 mm/s. Whereas, in the pinch-off regime, mean vortex velocity is about 800 mm/s and the pinch-off vortex velocity is around 1450 mm/s.
- 310 • Flickering frequency in the case of ethylene diffusion flame was measured by 11 Hz. This frequency is independent of injection velocity and follows St-Fr Sato's relation.
- A mechanical stabilizer was demonstrated to be efficient in stabilizing flickered diffusion flame for both fuels methane and ethylene. Stabilization depends on stabilizer geometry and its position.

- 315
- Numerical simulation shows the action of a stabilizer in air streamlines that could have an effect in enhancing stability: air streamlines appear smoother and more uniform with a mechanical stabilizer. This action is reduced when the stabilizer is mounted in a lower height.

Demonstrating the controllability of flickering by a mechanical actuator is a crucial result since this effect could be deployed at academic scale by extending the applicability domain of some techniques where a stable flame is needed (for example Rayleigh scattering/ extinction techniques to study particles formation in a flame [40]) or even could motivate designers in industrial scale to more consider the design of the external geometry and its effect on the aerodynamic around the flame. Nevertheless, this study could be followed by different actions: updating the model to consider transient physics like flickering is recommended to more clarify the effect of mechanical actuator. In the experimental part, the experimental parameters could be extended to cover larger applicability domain such as aeronautics by considering pressures above one atmosphere.

320

325

### **Declaration of Competing Interest**

330 The authors declare that they have no known competing financial interests or personal relationships that could have appeared to influence the work reported in this paper.

### **Acknowledgements**

The research reported in this publication was supported by labex Caprysses. (Convention ANR-11-LABX 0006-01). CNRS and Université d'Orléans. France.

### **Bibliography**

335

- [1] Fujisawa N. Nakashima K. Simultaneous measurement of three-dimensional flame contour and velocity field for characterizing the flickering motion of a dilute hydrogen flame. *Meas Sci Technol* 2007;18:2103–10. <https://doi.org/10.1088/0957-0233/18/7/041>.

- 340 [2] Fujisawa N. Okuda T. Effects of co-flow and equivalence ratio on flickering in partially  
premixed flame. *International Journal of Heat and Mass Transfer* 2018;121:1089–98.  
<https://doi.org/10.1016/j.ijheatmasstransfer.2018.01.072>.
- [3] Zhang D. Fang J. Guan J. Wang J. Zeng Y. Wang J. et al. Laminar jet methane/air  
diffusion flame shapes and radiation of low air velocity coflow in microgravity. *Fuel*  
345 2014;130:25–33. <https://doi.org/10.1016/j.fuel.2014.04.008>.
- [4] Fujisawa N. Matsumoto Y. Yamagata T. Influence of Co-flow on Flickering Diffusion  
Flame. *Flow Turbulence Combust* 2016;97:931–50. <https://doi.org/10.1007/s10494-016-9730-9>.
- [5] Gohari Darabkhani H. Wang Q. Chen L. Zhang Y. Impact of co-flow air on buoyant  
350 diffusion flames flicker. *Energy Conversion and Management* 2011;52:2996–3003.  
<https://doi.org/10.1016/j.enconman.2011.04.011>.
- [6] Wang Q. Gohari Darabkhani H. Chen L. Zhang Y. Vortex dynamics and structures of  
methane/air jet diffusion flames with air coflow. *Experimental Thermal and Fluid  
Science* 2012;37:84–90. <https://doi.org/10.1016/j.expthermflusci.2011.10.006>.
- 355 [7] Piemsinlapakunchon T. Paul MC. Effect of syngas fuel compositions on the occurrence  
of instability of laminar diffusion flame. *International Journal of Hydrogen Energy*  
2021;46:7573–88. <https://doi.org/10.1016/j.ijhydene.2020.11.259>.
- [8] Satyanarayana Raju P. Nayak GM. Balusamy S. Effect of Air Co-flow on Flickering  
Motion of LPG Laminar Diffusion Jet Flame. In: Prabu T. Viswanathan P. Agrawal A.  
360 Banerjee J. editors. *Fluid Mechanics and Fluid Power*. Singapore: Springer; 2021. p.  
717–25. [https://doi.org/10.1007/978-981-16-0698-4\\_79](https://doi.org/10.1007/978-981-16-0698-4_79).
- [9] Guahk YT. Lee DK. Oh KC. Shin HD. Flame-Intrinsic Kelvin–Helmholtz Instability of  
Flickering Premixed Flames. *Energy Fuels* 2009;23:3875–84.  
<https://doi.org/10.1021/ef900147x>.
- 365 [10] Sato H. Amagai K. Arai M. Flickering frequencies of diffusion flames observed under  
various gravity fields. *Proceedings of the Combustion Institute* 2000;28:1981–7.  
[https://doi.org/10.1016/S0082-0784\(00\)80604-9](https://doi.org/10.1016/S0082-0784(00)80604-9).
- [11] Darabkhani HG. Zhang Y. Methane Diffusion Flame Dynamics at Elevated Pressures.  
*Combustion Science and Technology* 2010;182:231–51.  
370 <https://doi.org/10.1080/00102200903418252>.
- [12] K. R. V. Manikantachari. Vasudevan Raghavan. K. Srinivasan. Natural Flickering Of  
Methane Diffusion Flames 2011. <https://doi.org/10.5281/ZENODO.1061856>.
- [13] Arai M. Sato H. Amagai K. Gravity effects on stability and flickering motion of  
diffusion flames. *Combustion and Flame* 1999;118:293–300.  
375 [https://doi.org/10.1016/S0010-2180\(98\)00159-X](https://doi.org/10.1016/S0010-2180(98)00159-X).
- [14] Aggarwal SK. Extinction of laminar partially premixed flames. *Progress in Energy and  
Combustion Science* 2009;35:528–70. <https://doi.org/10.1016/j.pecs.2009.04.003>.
- [15] Strawa AW. Cantwell BJ. Investigation of an excited jet diffusion flame at elevated  
pressure. *J Fluid Mech* 1989;200:309–36. <https://doi.org/10.1017/S0022112089000674>.
- 380 [16] Krikunova AI. Premixed methane-air flame under alternate gravity. *Acta Astronautica*  
2020;175:627–34. <https://doi.org/10.1016/j.actaastro.2020.04.054>.
- [17] Thirumalaikumaran SK. Vadlamudi G. Basu S. Insight into flickering/shedding in  
buoyant droplet-diffusion flame during interaction with vortex. *Combustion and Flame*  
2022;240:112002. <https://doi.org/10.1016/j.combustflame.2022.112002>.
- 385 [18] Chi Y. Yang T. Zhang P. Dynamical Mode Recognition of Triple Flickering Buoyant  
Diffusion Flames: from Physical Space to Phase Space and to Wasserstein Space 2022.  
<https://doi.org/10.48550/arXiv.2201.01085>.
- [19] Yang T. Chi Y. Zhang P. Vortex Interaction in Triple Flickering Buoyant Diffusion  
Flames 2022. <https://doi.org/10.48550/arXiv.2201.01585>.



- 390 [20] Hao G. Pang B. Zhang Q. Cui F. Sun S. Liu S. Flame synchronization and flow field  
analysis of double candles. *J Phys: Conf Ser* 2022;2247:012030.  
<https://doi.org/10.1088/1742-6596/2247/1/012030>.
- [21] Zhang J. Megaridis CM. Soot Microstructure in Steady and Flickering Laminar  
Methane/Air Diffusion Flames. *COMBUSTION AND FLAME* 1998;112:473–84.
- 395 [22] Wilson EL. Miller JH. Development of a pulsed sampling probe for time-resolved  
measurements in flickering flames. *Meas Sci Technol* 2001;12:1701–8.  
<https://doi.org/10.1088/0957-0233/12/10/313>.
- [23] Wang Q. Huang HW. Tang HJ. Zhu M. Zhang Y. Nonlinear response of buoyant  
diffusion flame under acoustic excitation. *Fuel* 2013;103:364–72.  
400 <https://doi.org/10.1016/j.fuel.2012.08.008>.
- [24] KERMIT C. SMYTH. JOEL E. HARRINGTON. JOHNSON EL. WILLIAM M.  
PITrS. Greatly Enhanced Soot Scattering in Flickering CH<sub>4</sub> Air Diffusion Flames.  
*COMBUSTION AND FLAME* 1993.
- [25] Ahn M. Yoon Y. Joo S. Effects of acoustic excitation on pinch-off flame structure and  
405 NO<sub>x</sub> emissions in H<sub>2</sub>/CH<sub>4</sub> flame. *International Journal of Hydrogen Energy*  
2022;47:13178–90. <https://doi.org/10.1016/j.ijhydene.2022.02.066>.
- [26] Shaddix CR. Harrington JE. Smyth KC. Quantitative measurements of enhanced soot  
production in a flickering methane/air diffusion flame. *Combustion and Flame*  
1994;99:723–32. [https://doi.org/10.1016/0010-2180\(94\)90067-1](https://doi.org/10.1016/0010-2180(94)90067-1).
- 410 [27] Dobashi R. Kong Z. Toda A. Takahashi N. Suzuki M. Hirano T. Mechanism Of Smoke  
Generation In A Flickering Pool Fire. *Fire Saf Sci* 2000;6:255–64.  
<https://doi.org/10.3801/IAFSS.FSS.6-255>.
- [28] Katta VR. Roquemore WM. Menon A. Lee S-Y. Santoro RJ. Litzinger TA. Impact of  
soot on flame flicker. *Proceedings of the Combustion Institute* 2009;32:1343–50.  
415 <https://doi.org/10.1016/j.proci.2008.06.152>.
- [29] Gotoda H. Kawaguchi S. Saso Y. Experiments on dynamical motion of buoyancy-  
induced flame instability under different oxygen concentration in ambient gas.  
*Experimental Thermal and Fluid Science* 2008;32:1759–65.  
<https://doi.org/10.1016/j.expthermflusci.2008.05.005>.
- 420 [30] Legros G. Gomez T. Fessard M. Gouache T. Ader T. Guibert P. et al. Magnetically  
induced flame flickering. *Proceedings of the Combustion Institute* 2011;33:1095–103.  
<https://doi.org/10.1016/j.proci.2010.06.124>.
- [31] Gillon P. Chahine M. Sarh B. Blanchard J-N. Gilard V. Stabilization of Lifted Laminar  
Co-Flow Flames by Oxygen-Enriched Air. *Combustion Science and Technology*  
425 2012;184:556–71. <https://doi.org/10.1080/00102202.2011.651230>.
- [32] Chahine M. Etude des effets magnétiques et des effets de l'enrichissement en oxygène  
sur la combustion d'une flamme de diffusion laminaire CH<sub>4</sub>-Air: optimisation de  
l'efficacité énergétique. These de doctorat. Orléans. 2012.
- [33] Delmaere T. Etude de l'effet d'un gradient de champ magnétique sur le développement  
430 de flammes de diffusion laminaires. These de doctorat. Orléans. 2008.
- [34] Gilard V. Gillon P. Blanchard J-N. Sarh B. Influence of a Horizontal Magnetic Field on  
a Co-Flow Methane/Air Diffusion Flame. *Combustion Science and Technology*  
2008;180:1920–35. <https://doi.org/10.1080/00102200802261506>.
- [35] Gillon P. Gilard V. Idir M. Sarh B. Electric field influence on the stability and the soot  
435 particles emission of a laminar diffusion flame. *Combustion Science and Technology*  
2019;191:325–38. <https://doi.org/10.1080/00102202.2018.1467404>.
- [36] Xiong Y. Lacoste DA. Chung SH. Cha MS. Effects of DC Electric Fields on Flickering  
and Acoustic Oscillations of an M-shape Premixed Flame. *Flow Turbulence Combust*  
2022;109:459–75. <https://doi.org/10.1007/s10494-022-00326-w>.

- 440 [37] Sato H. Amagai K. Arai M. Diffusion flames and their flickering motions related with  
Froude numbers under various gravity levels. *Combustion and Flame* 2000;123:107–18.  
[https://doi.org/10.1016/S0010-2180\(00\)00154-1](https://doi.org/10.1016/S0010-2180(00)00154-1).
- [38] Kashif M. Bonnetty J. Guibert P. Morin C. Legros G. Soot volume fraction fields in  
unsteady axis-symmetric flames by continuous laser extinction technique. *Optics*  
445 *Express* 2012;20:28742. <https://doi.org/10.1364/OE.20.028742>.
- [39] Sayed-Kassem A. Elorf A. Gillon P. Idir M. Sarh B. Gilard V. Numerical modelling to  
study the effect of DC electric field on a laminar ethylene diffusion flame. *International*  
*Communications in Heat and Mass Transfer* 2021;122:105167.  
<https://doi.org/10.1016/j.icheatmasstransfer.2021.105167>.
- 450 [40] Sayed-Kassem A. Gillon P. Idir M. Gilard V. On the Effect of a DC Electric Field on  
Soot Particles' Emission of a Laminar Diffusion Flame. *Combustion Science and*  
*Technology* 2019:1–12. <https://doi.org/10.1080/00102202.2019.1678901>.